Detection and limb brightening of the H I n=20–19 Rydberg line in the submillimetre spectrum of the Sun

T.A. Clark[1], D.A. Naylor[2], and G.R. Davis[3]

[1] Department of Physics and Astronomy, University of Calgary, Calgary, Alberta T2N 1N4, Canada (taclark@ucalgary.ca)
[2] Department of Physics, University of Lethbridge, Lethbridge, Alberta T1K 3M4, Canada (naylor@uleth.ca)
[3] Institute of Space and Atmospheric Studies, University of Saskatchewan, Saskatoon, Saskatchewan S7N 5E2, Canada (g.r.davis@usask.ca)

Abstract. Submillimetre spectra taken near to the solar limb with a polarizing interferometer on the James Clerk Maxwell Telescope have been compared with disk-centre spectra to reveal a limb-brightened feature whose peak intensity occurs at the predicted frequency of the n=20–19 Rydberg transition in H I at $29.622\,\mathrm{cm}^{-1}$. A shoulder on this peak, at $29.65\,\mathrm{cm}^{-1}$, has been tentatively assigned to the equivalent transition in Mg I. The H I line exhibits limb brightening of up to 9% of the disk-centre continuum intensity. The intensity of the Mg I line is about half of the H I line intensity across the observed region near to the limb. Widths of the H I line are between 0.020 and $0.027\,\mathrm{cm}^{-1}$, smaller than predicted by current models of this line in the Sun's spectrum. These measurements represent the highest-n Rydberg lines detected to date in the solar spectrum. The measured line intensity, line width, limb brightening and the relative heights of the contributions from H I and Mg I place constraints upon further modelling of the solar atmosphere.

Key words: line: identification – Sun: general – Sun: atmosphere – Sun: infrared

1. Introduction

Observations of high-n Rydberg transitions in the solar infrared spectrum have added a new dimension to the study of the solar photosphere and chromosphere over the last 20 years. This study began with the discovery of intense emission lines at $\sim12\,\mu$m (Murcray et al. 1981; Brault & Noyes 1983) and their identification as lines from n=7–6 Rydberg transitions of Mg I, Si I and Al I (Chang & Noyes 1983; Chang 1987). Subsequent ground-based investigations (e.g., Deming et al. 1988; Zirin & Bopp 1989; Hewagama et al. 1993) confirmed and extended the initial observations, particularly the strong limb brightening and high Zeeman sensitivity of the Mg I lines. Lines from the next highest Rydberg transition in both H I and Mg I (n=8–7 at $\sim20\,\mu$m) were detected in emission from Kitt Peak (Wallace et al. 1994), Jungfraujoch (Farmer et al. 1994) and Mauna Kea (Clark et al. 1994). Farmer et al. (1994) also observed the H I

n=9–8 line at $\sim28\,\mu$m. The ATMOS experiment on the Space Shuttle (Farmer & Norton 1989), unhindered by the terrestrial atmosphere, revealed a plethora of solar spectral features in the range 2.3–16 μm, most of which have now been attributed to transitions between levels up to n=10 in various atomic species. At longer wavelengths, far-infrared spectra taken at balloon altitudes (Boreiko & Clark 1986; Boreiko et al. 1994) revealed emission features from Rydberg transitions between high-n levels of H I (n=12–11 through 16–15) along with blended lines from equivalent hydrogenic transitions in heavier elements, predominantly Mg.

Many of these solar atomic transitions exhibited both absorption and emission components (Brault & Noyes 1983; Jefferies 1991), with emission becoming dominant towards the solar limb and at higher n values. Theoretical modelling successfully explained the general characteristics of both the H I and Mg I lines (H I: Carlsson & Rutten 1992; Mg I: Carlsson et al. 1992; Chang et al. 1991; Avrett et al. 1994) and demonstrated the potential value of these atomic lines as diagnostic probes of the photosphere-chromosphere boundary. In particular, the H I lines depend principally on the atmospheric temperature profile and appear to require a temperature inversion in the lower chromosphere, while the high Zeeman sensitivity of the Mg I and other metal lines make them potentially useful probes of the magnetic field structure.

The aim of the present experiment was to extend the range of measurements to higher-n Rydberg transitions and to explore the prospect of using such features in the study of the solar chromosphere (Naylor et al. 1994c). Some of these transitions occur in the submillimetre spectral range, in which observations are possible from high mountain sites through partially transmitting atmospheric windows. In this paper, following a preliminary announcement (Clark et al. 1995), we report the first detection and the limb brightening of the n=20–19 transition of H I at $29.622\,\mathrm{cm}^{-1}$.

2. Instrumentation and observations

The present observations were obtained with a dual-beam polarizing Fourier transform spectrometer (FTS) mounted at the Nasmyth focus of the James Clerk Maxwell Telescope (JCMT)

Send offprint requests to: T.A. Clark

in two observing runs in 1993 and 1998. The interferometer (Naylor et al. 1994b) was operated in rapid-scan mode, producing spectra with a resolution of $0.005\,\mathrm{cm}^{-1}$ in a scan time of one minute. The extended size of the Sun required that the interferometer be operated in single-beam mode, with one input port viewing the Sun and the second input port viewing a fixed-temperature blackbody source (Eccosorb AN 74, Emerson & Cuming).

The major difference in the instrumentation between the two observing runs was the detector system. In 1993, the JCMT facility bolometric detector, UKT14 (Duncan et al. 1990), was used. Several problems were encountered with this system: electrical pickup at the detector, extreme microphonic sensitivity, and the presence of several resonant optical cavities within the dewar which produced spectral fringing (Naylor et al. 1994a). Furthermore, since UKT14 was a single-bolometer system, only half of the radiation processed by the polarizing FTS was detected. In 1998, this detector was replaced by a new dual-polarization bolometer detector system (Naylor et al. 1999) which virtually eliminated common-mode electrical noise from the often-hostile telescope environment. The optical design of this system minimized the background radiant loading on the bolometer elements and the occurrence of resonant optical cavities.

In addition, different filters were used in the two observing runs. The wide-bandpass 350-μm filter internal to UKT14 was used in 1993. For the 1998 run, a narrowband filter, custom-designed for the range 28.8–$29.9\,\mathrm{cm}^{-1}$, was used to reduce the sensitivity to fluctuations in the atmospheric water vapour content.

To minimise the effects of variations in atmospheric transmission between scans, spectra were acquired in the following sequence: two at disk centre, two at a background sky position $2000''$ from disk centre, and two at a selected limb position. The cycle was repeated for various limb positions on both sides of the Sun over the range 840–$980''$ from disk centre, with all beam offsets made in azimuth to maintain constant airmass for each set of solar and sky spectra. Since both runs occurred between 0900 and 1100 local time in May (8 May 1993 and 26 May 1998), the solar geometry was such that limb observations were made near to the solar poles and thus avoided possible active regions at lower latitudes.

3. Data analysis

The raw interferograms were first screened for quality using software which automatically detected and allowed for the interactive removal of noise spikes, in particular those caused by cosmic ray impacts on the detector which contaminate roughly one in every ten interferograms. Standard Fourier transform spectroscopic analysis techniques were applied to the cleaned interferograms. The interferograms were 8 times oversampled to allow for the application of a digital filter prior to phase correction. Since the optical elements in the spectrometer and detector produced negligible dispersion over the narrow spectral range of interest, a linear phase correction was applied to each interferogram before Fourier transformation. The phase correction
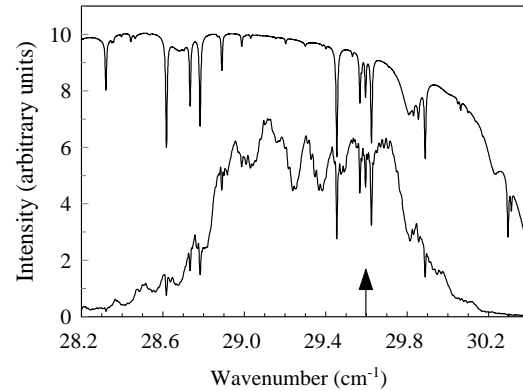
Fig. 1. The lower curve represents the average of two solar disk-centre spectra from the 1998 run. A synthetic atmospheric transmission spectrum, calculated for Mauna Kea and convolved to the $0.005\,\mathrm{cm}^{-1}$ spectral resolution of the interferometer, is superimposed for comparison (upper curve). The overall shape of the measured spectrum is controlled by a cooled narrowband filter, which is not included in the synthesis. The location of the H I n=20–19 feature is indicated.

function was determined by weighting phase values obtained from a short, double-sided interferogram by the amplitude of the corresponding spectral point (Forman et al. 1966).

Pairs of solar spectra were then averaged and the corresponding average background spectrum subtracted. Fig. 1 shows one such difference spectrum for the disk centre position along with a synthetic atmospheric transmission spectrum calculated for Mauna Kea using the spectral modelling program FASCOD (Anderson et al. 1996). The transmission spectrum has been convolved to a spectral resolution of $0.005\,\mathrm{cm}^{-1}$ to match the measured resolution of the interferometer (Naylor et al. 2000).

The structure in the measured spectrum in Fig. 1 arises from several sources: line absorption by atmospheric O_3, line and continuum absorption by atmospheric H_2O, the transmission characteristic of the narrow bandpass filter, and channel fringes generated by resonant optical cavities in the detector system. The combination of these effects, and their variability, makes identification of weak spectral features in the disk-centre solar spectrum difficult. Since lower-n Rydberg transitions are known to exhibit significant limb brightening, it was decided to search for the presence of a limb-brightened feature from the n=20–19 transition of H I by comparing limb and disk-centre spectra.

The dominant source of noise when observing near the solar limb is fluctuations in the apparent position of the Sun, resulting either from atmospheric turbulence (seeing) or from telescope tracking errors. The former is particularly problematic for daytime observations at Mauna Kea due to increased convective activity. The resulting modulation of the dc component of the interferogram, when Fourier transformed, can cause severe spectral distortion, both of the overall envelope and of the shape and depth of narrow features. Since three narrow O_3 lines lie in the vicinity of the H I line, any spectral distortion of these lines is particularly serious. We therefore limited this analysis to spectra obtained on days on which the atmosphere was both
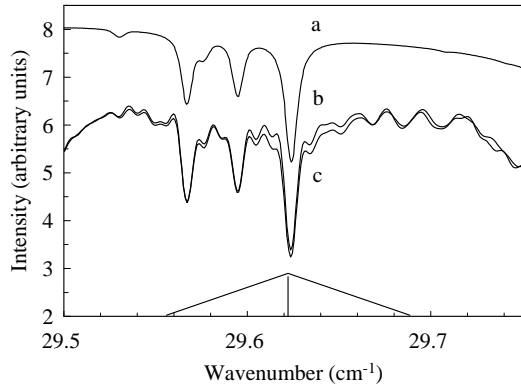
Fig. 2. Limb and disk-centre spectra (curves b and c, respectively). Excess emission, centred at 29.622 cm^{-1}, is clearly evident in the limb spectrum. A synthetic spectrum is also shown (curve a). The triangle indicates the predicted width and depth of the H I n=20–19 limb-brightened feature.

Fig. 3. The top trace shows a limb-to-centre difference spectrum following removal of the residual baseline. The limb-brightened emission feature is evident. The lower two curves represent fitted emission lines, and are offset for clarity.

dry and stable, as indicated by stability of the dc component of the interferogram.

Extracted portions of limb and disk-centre spectra, taken within minutes of each other, are compared in Fig. 2. After subtraction of the appropriate background, these spectra were scaled to match their continuum envelopes. The triangle indicates the predicted position and width of the H I feature. There is clear evidence of broad excess emission at the expected position. The emission feature was extracted from each limb spectrum by subtracting from it a scaled disk-centre spectrum, where the scaling factor was chosen to optimise the cancellation of the narrow ozone lines in the difference spectrum. This was found to be a sensitive technique and was justified by the good continuum cancellation achieved. Following subtraction, the small residual baseline was removed by spline-fitting to neighbouring regions of the difference spectrum. Standard spectroscopic fitting algorithms (GRAMS/32, Galactic Industries Corp.) were used with a combined Gaussian-Lorentzian line shape and fully variable fitting parameters to extract positions, heights and widths of component peaks from the excess emission feature.

4. Results and discussion

4.1. Line detection

Excess emission was found in all difference spectra taken in these two runs. An example is shown in Fig. 3, in which two components are clearly present. The main peak occurs at 29.621±0.005 cm^{-1}, in excellent agreement with the value for the H I n=20–19 transition (29.622 cm^{-1}). This transition has clearly been detected as excess limb emission, and represents the highest-n solar Rydberg transition reported to date. This approach gives a result which is ambiguous, however, since excess emission at the limb can arise either from limb brightening of an emission feature or from reduced absorption of an absorption feature. Previous observations of H I lines from transitions at n=8–7 (Wallace et al. 1994; Farmer et al. 1994; Clark et al. 1994), n=9–8 (Farmer et al. 1994) and the higher transitions 12–
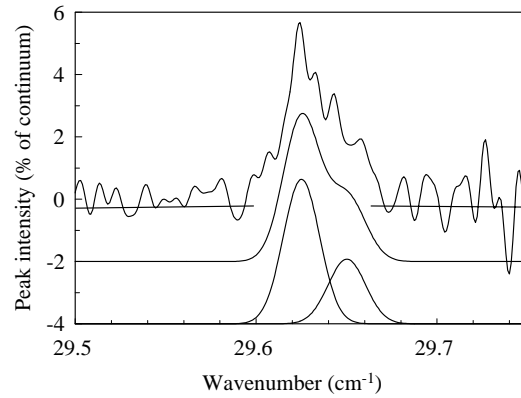
11 through 16–15 (Boreiko & Clark 1986; Boreiko et al. 1994) all show these lines in emission at disk-centre. Furthermore, the H I n=8–7 line shows limb brightening (Farmer, private communication; Clark et al. 1994) and the Mg I lines from n=7–6 transitions show considerable limb brightening. We therefore attribute this feature to a limb-brightened emission feature in the solar spectrum.

In principle, the observation of a distinct H I line from an atomic level as high as n=20 can place a limit on the electron density at the line source height since high electron density reduces the effective ionization energy of the atom and leads to broadening and blending of atomic energy levels. Kunc & Soon (1992) summarised calculations of these effects by several groups and showed that, under certain conditions, energy levels in atomic hydrogen can be blended at levels as low as n=11. Clearly, the detection of the present line indicates that atomic hydrogen energy levels are not blended to this level and that the effective ionization level is above n=20.

In fact, the detection of a line from level n=20 places no real constraint upon electron density since even the most conservative model merely sets an upper limit of $\sim$2x10^{13} cm^{-3}. This limit is two orders of magnitude higher than the expected electron density of 1.2x10^{11} cm^{-3} in the MACKKL atmospheric model (Maltby et al. 1986) at the predicted line source height of $\log \tau_{0.5} = -4.08$ (Carlsson & Rutten 1992). These models predict that energy level blending will only become effective at around n=40, which is consistent with the present observations.

A wider and less-intense feature was also detected at 29.65±0.01 cm^{-1}, as shown in Fig. 3. The most likely origin of this line is a blend of lines from the n=20–19, $\ell = n - 1$, $n - 2, \cdots$ transitions of Mg I at 29.638 cm^{-1}, and we make this tentative assignment for the remainder of this paper. In practice, however, the feature is probably a blend of Mg I transitions with weaker lines from heavier elements, the most likely of which, on the basis of near-infrared observations and the theoretical predictions of Carlsson et al. (1992), would be Si I.
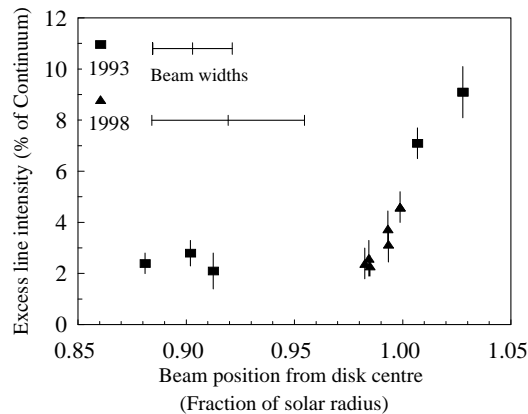
Fig. 4. Peak height of the H I n=20–19 excess emission as a function of the position of the centre of the telescope beam, represented as a fraction of the submillimetre solar radius. This radius was 953.4″ for the 1993 run and 949.6″ for the 1998 run, these values including the small submillimetre limb extension of 2.5″ beyond the visible limb (Clark et al. 1992). The two points which lie beyond the limb represent the sampling of the extreme limb by a portion of the wide beam of the telescope. The approximate telescope beam widths for these two runs are also shown.

4.2. Limb brightening

Fig. 4 shows the limb-brightening curve of the peak intensity of the H I excess emission. Each of these measurements represents a convolution of line emission over the solar disk with the beam pattern of the telescope, centred at the appropriate limb position. Data points which are apparently off the Sun actually represent samples of the extreme solar limb by the wide telescope beam. Under solar illumination, the telescope beam was found to have two components: a diffraction-limited core and an extended pedestal (Lindsey & Roellig 1991; Clark et al. 1992) with a width greater than 100″ which accounts for as much as 70% of the beam sensitivity. There is clear evidence of intense limb brightening in this feature very near to the limb. This is consistent with limb brightening characteristics for other infrared wavelengths and atomic species (H I, n =8–7, Farmer, private communication; Clark et al. 1994; Mg I, n=7–6, Brault & Noyes 1983). Fig. 5 shows the equivalent curve for the Mg I feature, which again shows clear limb brightening close to the extreme limb.

4.3. Line intensities

There have been few observations of H I lines at high n values. The intensities of the observed lines are compared with theoretical predictions from several models in Fig. 6. Although the disk-centre intensity of the H I n=20–19 line was not determined by the differencing technique employed in the present work, an extrapolated value was estimated by following the trend observed in lower-n transitions. Hoang-Binh (1982) used various approximations and the VAL 3C atmospheric model (Vernazza et al. 1981) to calculate LTE line intensity estimates by numerical integration. Carlsson & Rutten (1992) used the
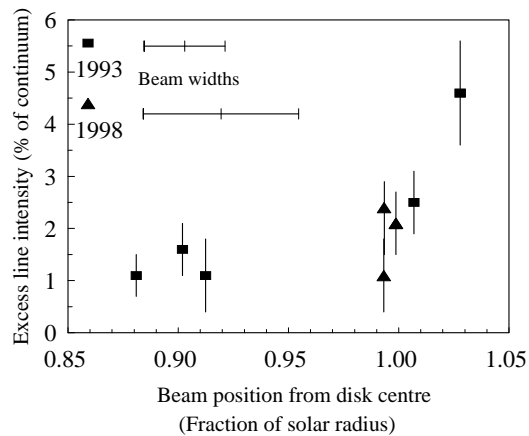
Fig. 5. Peak height of the Mg I n=20–19 excess emission as a function of the position of the centre of the telescope beam, determined as in Fig. 4.

improved MACCKL atmospheric model (Maltby et al. 1986) and more rigorous modelling to produce a full, self-consistent solution to predict H I line intensities. From this work, they concluded that the experimental data lay between the predictions from their radiative atmosphere model without chromosphere, which predicts essentially no H I emission at higher n values, and those from their NLTE and LTE atmospheric models. The present result is in line with this conclusion. They suggested that agreement between theory and experiment must await an accurate description of the ill-defined bifurcation of the Sun's atmosphere in which a narrow network of hot, magnetic gas, the chromospheric network, surrounds larger regions of cooler gas, the supergranular cells. Conditions within these cooler regions are controlled, at least in part, by the formation of robust molecules such as CO and OH which radiate strongly upon formation, and efficiently cool their surroundings (Ayres 1981, 1991).

Another parameter of interest when comparing theoretical predictions with observations is the ratio of Mg I to H I line intensity. For n=12–11 and 13–12 in the far-infrared balloon data (Boreiko et al. 1994), where the Mg I lines are distinct from the H I lines, this ratio is 0.87 and 0.70 respectively. The ratio of Mg I to H I line intensity in the present data, taken near the solar limb, is ∼0.5. This general trend, in which the intensity ratio decreases with wavelength, was predicted by Carlsson et al. (1992).

4.4. Line widths

The widths of the H I lines show considerable scatter, but lie between 17 and 27 mK (1 mK = 10^{-3} cm^{-1}) and show a slight trend towards increased widths at the extreme limb. These values are below the prediction of 35 mK by Hoang-Binh in his original paper (Hoang-Binh 1982) and even further below the more refined prediction of 40 mK in a later paper (Hoang-Binh et al. 1987). This discrepancy is important because line broad-
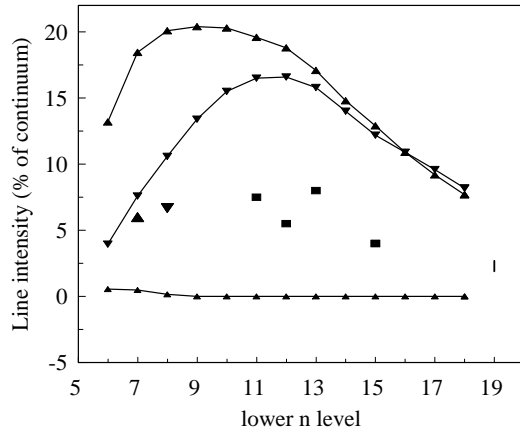
Fig. 6. Predicted and observed intensities of solar H I Rydberg lines are shown as a function of lower quantum number. The two upper curves represent the NLTE (top) and LTE calculations of Carlsson & Rutten (1992). Both utilize the MACKKL atmospheric model (Maltby et al. 1986) which includes a temperature inversion and a hot chromosphere. The bottom curve is the Carlsson-Rutten model for a radiative atmosphere with no chromosphere. The observations include: the n=7–6 line detected by ATMOS (Farmer & Norton 1989), denoted by the oval; the n=8–7 line measured from mountain altitude sites by Farmer et al. (1994) and Wallace et al. (1994), denoted by a triangle; the n=9–8 line measured by Farmer et al. (1994), denoted by an inverted triangle; and the balloon-borne measurements of Boreiko et al. (1994), denoted by squares. The present result for the n=20–19 transition, extrapolated to disk centre for comparison, is shown; the vertical bar represents an estimate of the uncertainty in the extrapolation.

ening at the line source height is known to control the peak intensity of the resulting line (Carlsson & Rutten 1992).

One possible explanation for this discrepancy is that the line fitting procedure is sensitive to the assumed baseline and may have concealed wide Lorentzian wings of these emission lines. Hoang-Binh (1982) provided a perceptive warning about the difficulty of detecting the wide line wings which he predicted for higher n transitions. Thus, these line widths, and to a lesser extent the reported line intensities, may be underestimated and describe the narrower Doppler cores of the actual emission lines. Certainly, there is evidence of wide Lorentzian wings on the n=12–11 and 13–12 lines in the balloon data of Boreiko et al. (1994), and these lines appear to have widths of about 40 mK, significantly higher than predicted widths for these transitions. This will be an important consideration in future work, particularly because the formation of the H I line, as described by Rutten & Carlsson (1994), arises from two distinctly different regions of the solar atmosphere: the line core from the lower chromosphere, and the wide wings from the denser lower photosphere. Identification and measurement of the two components would provide a valuable diagnostic tool for the further evaluation of the structure of the solar atmosphere.

The Mg I line widths, while more difficult to estimate, also show considerable scatter but lie between 19 and 42 mK. There is a trend towards higher values as the limb is approached, the highest value being for the point at the extreme limb. The signif-

icance of these values is probably low because of the composite nature of this feature.

5. Conclusions

The present observations near to the limb of the Sun have demonstrated the existence of emission from the n=20–19 Rydberg transition in H I at 29.622 cm^{-1} in the submillimetre solar spectrum whose intensity exceeds that at disk-centre by 2–9% of the continuum intensity level. A second component has been identified on the shoulder of this line at 29.65 cm^{-1}, which we attribute to the equivalent n=20–19 Rydberg Mg I transition. Both components show significant limb brightening.

Future work on these and similar lines will have to overcome some of the difficulties outlined in this paper. The next highest line which lies within a reasonable atmospheric window accessible from the JCMT is the n=22–21 transition at 22.095 cm^{-1} in the 450 μm atmospheric window. The JCMT has a better beam pattern and efficiency at this wavelength (Clark et al. 1992), making measurements near to the solar limb easier. The expected intensity of this and higher n Rydberg transitions is much smaller than for the present line, however, making their detection more difficult (Fig. 6). Furthermore, extraction of the expected wide wings of these lines will be even more challenging. Nevertheless, if such lines can be detected, the diffraction limited beam of the JCMT is sufficiently narrow to allow the search for enhanced line emission from the hot chromospheric network. The protective screen and spatial resolution provided by the JCMT make it the only facility capable of such observations.

References

Anderson G.P., Kneizys F.X., Chetwynd J.H., et al., 1996, SPIE 2830, 82

Avrett E.H., Chang E.S., Loeser R., 1994, In: Rabin D.M., Jefferies J.T., Lindsey C.A. (eds.) Proc. IAU Symp. 154, Infrared Solar Physics. Kluwer, Dordrecht, p. 323

Ayres T.R., 1981, ApJ 244, 1064

Ayres T.R., 1991, In: Ulmschneider P., Priest E.R., Rosner R. (eds.) Proc. Mechanisms of Chromospheric and Coronal Heating. Springer-Verlag, Berlin, p. 228

Brault J., Noyes R.W., 1983, ApJ 269, L61

Boreiko R.T., Clark T.A., 1986, A&A 157, 353

Boreiko R.T., Clark T.A., Naylor D.A., et al., 1994. In: Rabin D.M., Jefferies J.T., Lindsey C.A. (eds.) Proc. IAU Symp. 154, Infrared Solar Physics. Kluwer, Dordrecht, p. 367

Carlsson M., Rutten R.J., 1992, A&A 259, L53

Carlsson M., Rutten R.J., Shchukina N.G., 1992, A&A 253, 567

Chang E.S., 1987, Phys. Scripta 35, 792

Chang E.S., Noyes R.W., 1983, ApJ 275, L11

Chang E.S., Avrett E.H., Mauas P.J., et al., 1991, ApJ 379, L79

Clark T.A., Naylor D.A., Tompkins G.J., et al., 1992, Solar Phys. 140, 393

Clark T.A., Naylor D.A., Tompkins G.J., 1994, In: Caillault J.-P. (ed.) Proc. ASP Conference Series 64, p. 608

Clark T.A., Naylor D.A., Davis G.R., 1995, In: Kuhn J.R., Penn M.J. (eds.) Proc. 15th NSO/SP Summer Workshop, IR Tools for Solar Astrophysics: What's Next? World Sci. Publ. Co. Ltd., p. 139

Deming D., Boyle R.J., Jennings D.E., Wiedemann G., 1988, ApJ 333, 978

Duncan W.D., Robson E.I., Ade P.A.R., et al., 1990, MNRAS 243, 126

Farmer C.B., Norton R.H., 1989, NASA Ref. Pub. 1224

Farmer C.B., Delbouille L., Roland G., et al., 1994, San Juan Capistrano Research Institute Technical Report 94-2

Forman M.L., Steel W.H., Vanasse G.A., 1966, J. Opt. Soc. Am. 56, 59

Hewagama T., Deming D., Jennings D.E., et al., 1993, ApJS 86, 313

Hoang-Binh D., 1982, A&A 112, L3

Hoang-Binh D., Brault P., Picart J., et al., 1987, A&A 181, 134

Jefferies J.T., 1991, ApJ 377, 337

Kunc J.A., Soon W.H., 1992, ApJ 296, 364

Lindsey C.A., Roellig T.L., 1991, ApJ 375, 414

Maltby P., Avrett E.H., Carlsson M., et al., 1986, ApJ 306, 284

Murcray F.J., Goldman A., Murcray F.H., et al., 1981, ApJ 247, L97

Naylor D.A., Davis G.R., Griffin M.J., et al., 1994a, A&A 291, L51

Naylor D.A., Tompkins G.J., Clark T.A., et al., 1994b, SPIE 2198, 703

Naylor D.A., Tompkins G.J., Clark T.A., et al., 1994c, In: Rabin D.M., Jefferies J.T., Lindsey C.A. (eds.) Proc. IAU Symp. 154, Infrared Solar Physics. Kluwer, Dordrecht, p. 323

Naylor D.A., Gom B.G., Ade P.A.R., et al., 1999, Rev. Sci. Inst. 70, 4097

Naylor D.A., Davis G.R., Gom B.G., et al., 2000, MNRAS, in press

Rutten R.J., Carlsson M., 1994. In: Rabin D.M., Jefferies J.T., Lindsey C.A. (eds.) Proc. I.A.U. Symp. 154, Infrared Solar Physics. Kluwer, Dordrecht, p. 309

Vernazza J.E., Avrett E.H., Loeser R., 1981, ApJS 45, 635

Wallace L., Livingston W.C., Bernath P., 1994, NSO Technical Report 1994-01

Zirin H., Bopp B., 1989, ApJ 340, 571